

Comparison of Polybinary Shaping and Tomlinson Harashima Precoding under Brick-wall Bandwidth Constraint

Yixiao Zhu, Qunbi Zhuge, and Weisheng Hu

State Key Laboratory of Advanced Optical Communication System and Networks, Shanghai Jiao Tong University, 800 Dongchuan Rd, Shanghai, 200240, China, yixiaozhu@sjtu.edu.cn

Abstract We experimentally compare polybinary shaping and Tomlinson-Harashima precoding (THP) under 25GHz brick-wall bandwidth limitation, achieving 120%, 50% and 20% faster-than-Nyquist rates with 110Gbaud OOK, 75Gbaud PAM-4 and 60Gbaud PAM-6. Results indicate that polybinary shaping outperforms THP with OOK, while THP is better for higher-order formats. ©2022 The Author(s)

Introduction

There is continuously growing capacity demand in data-center interconnects (DCI) driven by the emerging bandwidth-hungry applications such as high-definition video, blockchain, and cloud computing. As the Ethernet inference is evolving from 400GbE to 800G implemented by 4 intensity-modulation direct-detection (IM-DD) lanes with 200Gb/s bitrate^[1], the bandwidth requirement on both modulator and digital-to-analogue convertor (DAC) becomes challenging.

Faster-than-Nyquist (FTN) technique have been considered as a promising solution to transmit more bits in bandwidth-limited channel. One typical approach is binary precoding^[2], which introduces controlled inter-symbol interference (ISI) as a low-pass filter. Such spectrally shaping can alleviate the influence of bandwidth limitation thanks to the reduced signal bandwidth. With cascaded binary precoder, i.e. polybinary shaping, more signal energy can be concentrated into the low-frequency regime, leading to much stronger tolerance. In the sampling-rate-limited scenario, 210Gbaud on-off keying (OOK) signal can be generated based on 120GSa/s DAC with 7-order polybinary shaping^[3]. For 100Gb/s 4-ary pulse amplitude modulation (PAM-4) transmission, 2-order binary shaping can help reach the 20% hard-decision forward error correction (HD-FEC) threshold^[4] of 1.5×10^{-2} under 19GHz brick-wall bandwidth limitation, corresponding to FTN rate of 31.6%^[5]. Here FTN rate is defined as the ratio between excess Nyquist bandwidth of transmitted signal by system bandwidth, i.e. $(B_{Nyquist}/B_{system} - 1)$. More recently, by applying 8-order partial response signalling, up to 310Gbaud OOK generation is reported with 128GSa/s DAC^[6].

On the other hand, Tomlinson-Harashima precoding (THP)^[7,8] is also an effective solution for FTN transmission. Since conventional feed-forward equalizer (FFE) cannot fully mitigate the severe ISI in FTN transmission, decision-feedback equalizer (DFE) is designed to cope

with the spectral nulls. Considering the error-propagation effect caused by decision error, DFE is moved to the transmitter as THP to process the original symbol sequences. With numerically calculated coefficients, 21.73% FTN rate and spectral efficiency of 4.30b/s/Hz is reported with single-polarization 28Gbaud 16-ary quadrature amplitude modulation (16-QAM)^[9]. Remarkably, under 33GHz brick-wall bandwidth constraint, up to 94Gbaud PAM-4 can be successfully transmitted over 2km standard single-mode fiber (SSMF) at record 42.4% FTN rate^[10].

In this work, we experimentally compare the performance of polybinary shaping and THP under 25GHz brick-wall bandwidth limitation. The extended constellation, peak-to-average power ratio (PAPR), signal spectrum and BER after precoding are comprehensively evaluated with OOK, PAM-4 and PAM-6 formats, respectively. It is observed that for OOK signal, polybinary shaping outperforms THP, while THP shows its advantage with PAM-4 and higher formats. After 1km SSMF transmission, 110Gbaud OOK with polybinary shaping, 75Gbaud PAM-4 and 60Gbaud PAM-6 signal with THP can reach the 20% HD-FEC threshold, corresponding to FTN rate of 120%, 50% and 20%, respectively.

Principle

Figure 1(a) and 1(b) illustrate the structure of polybinary shaping and THP. For polybinary shaping, which is also referred as partial response signalling, the input symbol sequence is delayed by an integer number of symbol period and added as a finite impulse response (FIR) filter. For N -order polybinary shaping, the taps a_i can be straightforwardly obtained according to the coefficient of N -order polynomial $(1 + D)^N$.

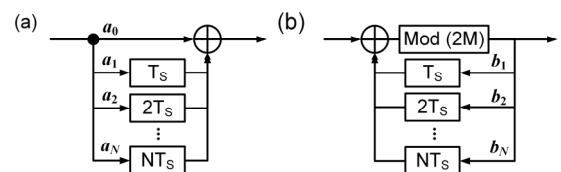


Fig. 1: Structure of (a) Polybinary shaping and (b) THP.

The induced ISI can be eliminated with maximum likelihood sequence detection (MLSD) at the receiver with the same coefficients. With M -ary modulation alphabet, M^N states need to be traversed for minimum Euclidean distance path searching, indicating exponential computational complexity growth with polybinary order. For THP approach, the input symbol sequence is added with precoder output, whose amplitude is constrained by modulo operation. The additional complexity is coefficient estimation with DFE based on training sequence through end-to-end measurement in advance. At the receiver, the extended pattern can be easily collapsed into original constellation after applying another modulo operation.

Experimental Setup

Figure 2(a) shows the experimental setup and DSP stacks. At the transmitter, OOK, PAM-4 and PAM-6 symbol sequences are mapped from binary bit streams. 30 taps are used in THP to cover the ISI length. After precoding, the symbol sequence is up-sampled and shaped with 0.01 roll-off root-raised cosine (RRC) filter. Then a digital brick-wall filter is implemented in the frequency domain to emulate 25GHz strict bandwidth constraint. Afterwards, the waveform is down-sampled to desired symbol rate and send to arbitrary waveform generator (AWG, Keysight M8194) operating at 120GSa/s. The electrical waveform is amplified by 50GHz electrical amplifier (EA) and modulated onto optical carrier at 1550nm through 40GHz electro-absorption modulator (EAM). The bias voltage is optimized as -0.8V with 120mV Vpp considering the linear modulation region in Fig.2(b). The 10dB

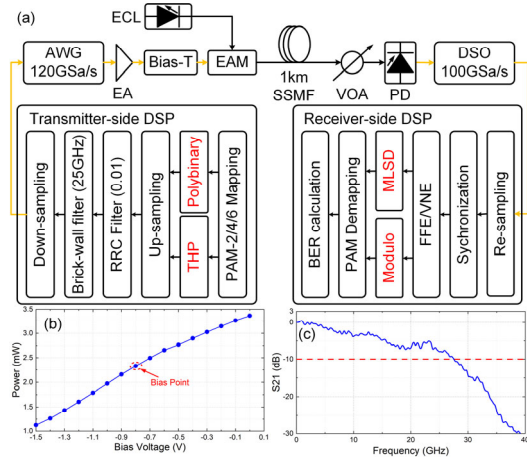


Fig. 2: (a) Experimental setup, transmitter- and receiver-side DSP. AWG: arbitrary waveform generator; EA: electrical amplifier; ECL: external cavity laser; EAM: electro-absorption modulator; SSMF: standard single-mode fiber; VOA: variable optical attenuator; PD: photodiode; DSO: digital storage oscilloscope; RRC: root-raised cosine; FFE: feed-forward equalizer; VNE: Volterra nonlinear equalizer. (b) Measured output optical power versus bias voltage of EAM. (c) Measured end-to-end S21 response.

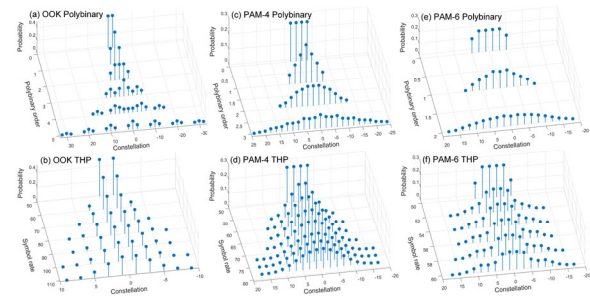


Fig. 3: Extended constellation distributions of (a) OOK, (c) PAM-4, and (e) PAM-6 with polybinary shaping, respectively. Extended constellation distributions of (b) OOK, (d) PAM-4, and (f) PAM-6 with THP, respectively.

bandwidth of the system is measured as 27.6GHz. The fiber link is 1km SSMF to cover the DR requirement. At the receiver, received optical power is fixed as 1dBm by a variable optical attenuator (VOA). The optical signal is detected by 40GHz photodiode (PD) and captured by 100GSa/s digital storage oscilloscope (DSO, Tektronix DPO75902SX). In the offline DSP, the waveform is firstly re-sampled to 2 samples-per-symbol. After synchronization, linear FFE and sparse Volterra nonlinear equalizer (VNE) are employed updated by recursive least square (RLS) algorithm based on extended constellations after precoding. The 1st-, 2nd- and 3rd-order taps are 401, 33 and 17, respectively. With MLSD or modulo operation, the PAM symbols are finally recovered and BER is calculated by averaging 1.5×10^5 bits.

Results and Discussions

Fig.3(a)-3(f) display the extended constellation distributions with polybinary shaping or THP, respectively. Both precoding schemes lead to extended constellation to deal with the reduced bandwidth. Specifically, the maximum eye level is almost doubled with a higher polybinary order, making it more vulnerable to link nonlinearity. In comparison, the distribution of constellation points spread out more slowly with THP.

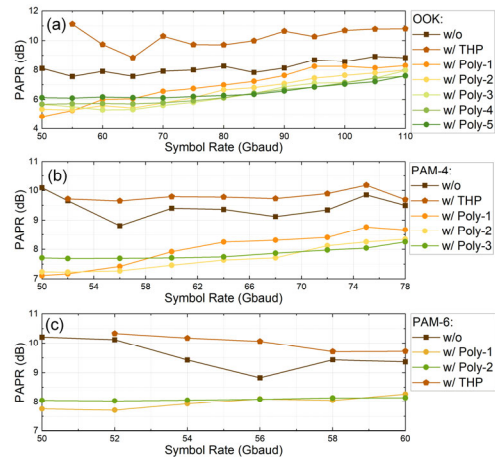


Fig. 4: PAPR of (a) OOK, (b) PAM-4, and (c) PAM-6 signal with polybinary shaping and THP, respectively. w/o: without precoding; w/ with; Poly-1: 1-order polybinary shaping.

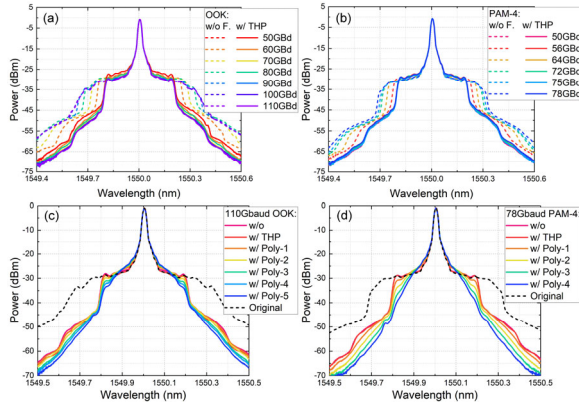


Fig. 5: Optical spectra of (a) OOK with THP; (b) PAM-4 with THP; (c) 110Gbaud OOK and (d) 78Gbaud PAM-4 with precoding. w/o F.: without brick-wall filter; w/ Poly-k: with k-order polybinary shaping.

Fig.4(a)-4(c) show the PAPR of precoded OOK and PAM-4/6 waveforms, respectively. It can be found that polybinary shaping can significantly lower the PAPR because its distribution is flatter. The PAPR gradually increases as bandwidth limitation becomes more severe. In contrast, THP slightly enhances the PAPR, which would result in SNR loss under peak power constraint in amplifier-less link.

Fig.5(a) and 5(b) show the measured optical spectra without digital brick-wall filter and with THP at 0.02nm resolution. The dashed curves correspond to original spectra without bandwidth limitation as reference. It is observed that the OOK and PAM-4 signals are successfully constrained into rectangular-like spectra, occupying $\sim 0.4\text{nm}$ optical bandwidth (50GHz equivalently for double-sideband signal). Fig.5(c) and 5(d) compare the spectra with different precoding schemes. As the polybinary shaping order increases, the low-frequency components around optical carrier rises while the high-frequency parts are further suppressed.

Fig.6(a)-6(c) compare the BER performance versus symbol rate for OOK and PAM-4/6 signals

under 25GHz brick-wall bandwidth constraint with polybinary shaping or THP after 1km SSMF transmission, respectively. By comparing FFE and VNE curves, higher error floor and larger nonlinear penalty can be observed with higher polybinary orders, which comes from the increased number of eye levels. After applying VNE, 60, 80, 90, 95, 105, and 110Gbaud OOK can reach the 20% HD-FEC threshold of 1.5×10^{-2} with 0/-1/-2/-3/-4/-5-order polybinary shaping, respectively. Although THP can also support 110Gbaud OOK transmission, the overall BER performance is worse than 5-order polybinary shaping. For PAM-4 format as in Fig.6(b), 1-order polybinary should be chosen until 60Gbaud, and 3-order gradually becomes better for 70Gbaud and beyond. Nevertheless, the BERs of THP are always lower than polybinary shaping. If 20% soft-decision (SD-) FEC threshold of 2×10^{-2} is adopted, 78Gbaud PAM-4 transmission is still available, which equals to 56% FTN rate. For PAM-6 signal transmission, the gap between polybinary shaping and THP is further enlarged, revealing that THP is more suitable for high-order format FTN transmission.

Conclusions

In conclusion, polybinary shaping and THP are experimentally compared for FTN transmission in a strictly bandwidth-limited IM-DD link. We reveal that polybinary shaping can outperform THP with OOK format, and THP becomes more advantageous with higher formats of PAM-4 and PAM-6. Under 25GHz brick-wall bandwidth constraint, 110Gb/s (110Gbaud) OOK, 150Gb/s (75Gbaud) PAM-4 and 150Gb/s (60Gbaud) PAM-6 can be successfully transmitted, resulting in FTN rate of 120%, 50% and 20%, respectively. Our work provides a potential reference for high-speed DCI links using low-cost transceivers.

Acknowledgements

This work was supported by NSFC (62001287).

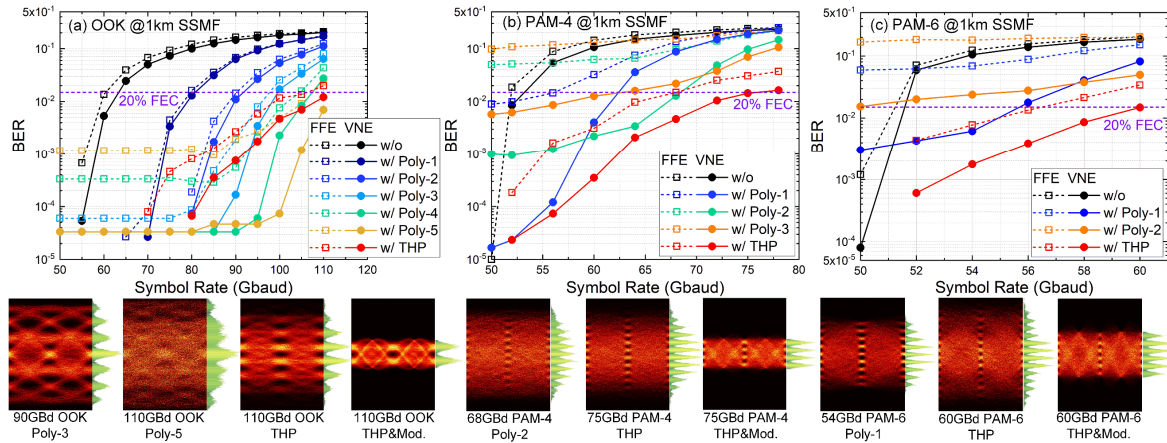


Fig. 6: Measured BER versus symbol rate of (a) OOK, (b) PAM-4, and (c) PAM-6 with polybinary shaping and THP under 25GHz bandwidth limitation after 1km transmission, respectively. w/o: without; w/ Poly-k: with k-order polybinary shaping.

References

- [1] X. Zhou, R. Urata and H. Liu, "Beyond 1 Tb/s intra-data center interconnect technology: IM-DD or coherent?," *Journal of Lightwave Technology*, vol. 38, no. 2, pp. 475–484, Jan. 2020, DOI: [10.1109/JLT.2019.2956779](https://doi.org/10.1109/JLT.2019.2956779)
- [2] Q. Zhang, N. Stojanovic, C. Prodaniuc, C. Xie, M. Koenigsmann, and P. Laskowski, "Single-lane 180 Gbit/s PAM-4 signal transmission over 2 km SSMF for short-reach applications," *Optics Letters*, vol. 41, no. 19, pp. 4449–4452, 2016, DOI: [10.1364/OL.41.004449](https://doi.org/10.1364/OL.41.004449)
- [3] Y. Zhu, X. Fang, L. Zhang, F. Zhang, and W. Hu, "Sub-sampling generation of ultra-high baud rate PAM/QAM signals via high-order partial response narrowing," *Optics Express*, vol. 29, no. 26, pp. 44063–44079, 2021, DOI: [10.1364/OE.442939](https://doi.org/10.1364/OE.442939)
- [4] L. M. Zhang, and F. R. Kschischang, "Staircase Codes With 6% to 33% Overhead," *Journal of Lightwave Technology*, vol. 32, no. 10, pp. 1999–2002, 2014, DOI: [10.1109/JLT.2014.2316732](https://doi.org/10.1109/JLT.2014.2316732)
- [5] Q. Wu, Y. Zhu, L. Yin, and W. Hu, "50 Gbaud PAM-4 IM-DD transmission with 24% bandwidth compression based on polybinary spectral shaping," 47th European Conference on Optical Communication (ECOC), 2021, We3C2.3, DOI: [10.1109/ECOC52684.2021.9606146](https://doi.org/10.1109/ECOC52684.2021.9606146)
- [6] M. S.-B. Hossain, T. Rahman, N. Stojanović, F. Pittalà, S. Calabrò, G. Böcherer, T. Wettlin, J. Wei, C. Xie, M. Kuschnerov, and S. Pachnicke, "Partial Response O-band EML Transmission Beyond 300-GBd with a 128/256 GSa/s DAC," *Optical Fiber Communication Conference (OFC) 2022, M2H.1*, DOI: [10.1364/OFC.2022.M2H.1](https://doi.org/10.1364/OFC.2022.M2H.1)
- [7] M. Tomlinson, "New automatic equalizer employing modulo arithmetic," *Electronics Letters*, vol. 7, no. 5, pp. 138–139, 1971, DOI: [10.1049/el:19710089](https://doi.org/10.1049/el:19710089)
- [8] H. Harashima and H. Miyakawa, "Matched-transmission technique for channels with intersymbol interference," *IEEE Transactions on Communications*, vol. 20, no. 4, pp. 774–780, 1972, DOI: [10.1109/TCOM.1972.1091221](https://doi.org/10.1109/TCOM.1972.1091221)
- [9] S. An, J. Li, X. Li, and Y. Su "FTN SSB 16-QAM Signal Transmission and Direct Detection Based on Tomlinson-Harashima Precoding With Computed Coefficients," *Journal of Lightwave Technology*, vol. 39, no. 7, pp. 2059–2066, 2021, DOI: [10.1109/JLT.2020.3046717](https://doi.org/10.1109/JLT.2020.3046717)
- [10] Q. Hu, M. Chagnon, K. Schuh, F. Buchali, and H. Bülow, "IM/DD Beyond Bandwidth Limitation for Data Center Optical Interconnects," *Journal of Lightwave Technology*, vol. 37, no. 19, pp. 4940–4946, 2019, DOI: [10.1109/JLT.2019.2926218](https://doi.org/10.1109/JLT.2019.2926218)